Optical conductivity of $Ba_{1-x}K_xBiO_3$ through the metal-semiconductor transition

M. A. Karlow, S. L. Cooper, A. L. Kotz,* and M. V. Klein
Department of Physics, Materials Research Laboratory, University of Illinois at Urbana-Champaign, 104 South Goodwin Avenue, Urbana, Illinois 61801

P. D. Han and D. A. Payne
Department of Materials Science and Engineering, Materials Research Laboratory, University of Illinois at Urbana-Champaign, 104 South Goodwin Avenue, Urbana, Illinois 61801

(Received 14 December 1992; revised manuscript received 6 May 1993)

The dielectric response of $Ba_{1-x}K_xBiO_3$ (BKBO) is investigated via room-temperature optical reflectance and spectroellipsometry over the doping range $0 \le x \le 0.51$. We find that with *increasing* x, (i) a semiconductor-to-metal (MS) transition occurs near $x = 0.35$, (ii) the infrared absorption band decreases monotonically in energy and persists into the metallic regime, and (iii) the integrated optical conductivity between 0 and 4 eV increases below the MS transition, but decreases above the MS transition. The decrease in the infrared absorption band energy suggests a relaxation of the distorted oxygen octahedra toward equilibrium with increasing x, and the doping dependence of the integrated optical conductivity is consistent with a crossover from holelike carriers below the MS transition to electronlike carriers above. A self-consistent interpretation of these results is provided by a general *bond-order* charge-density-wave model in which deviations of the Bi-O bond length from equilibrium influence many aspects of the normal-state response. We discuss the implications of this interpretation for BKBO and $BaPb_yBi_{1-y}O_3$.

I. INTRODUCTION

The normal-state properties of the bismuthate superconductors, $Ba_{1-x}K_xBiO_3$ (BKBO) and $BaPb_yBi_{1-y}O_3$ (BPBO), are dominated by doping-induced semiconductor-to-metal (MS) transitions near $x = 0.35$ (Ref. 1) and $y = 0.70$.[2] Although these transitions have been studied extensively, the persistence of semiconductivity away from half filling ($x = y = 0$) has proven difficult to explain theoretically. For example, band-structure calculations[3–6] fail to anticipate any semiconducting regime, predicting instead a metallic state for both materials at all doping levels. Tight-binding models[3,7] account for the semiconductivity only at half filling where perfectly nested electron and hole Fermi surfaces stabilize a commensurate three-dimensional charge-density wave (CDW), and open a semiconducting gap at the Fermi energy. However, away from half filling, tight-binding models[3,7] predict metallic behavior because the added carriers lift the nesting degeneracy and destabilize the CDW state. In order to account for the persistence of semiconductivity away from half filling, several novel mechanisms have been proposed, including chemical ordering waves,[8] site potential differences,[9] real-space electron pairing (small bipolarons),[10,11] and ordering of localized holes.[12] Unfortunately, an absence of wide-range doping dependence studies has made it impossible to critically test important predictions of these models.

This paper presents the first optical reflectance and spectroellipsometric measurements of single-crystal BKBO. These optical investigations cover a wider range of doping ($0 \le x \le 0.51$) than previously reported,[13,14] providing a detailed picture of the doping dependence of the normal-state optical response of BKBO through the MS transition. A number of trends are observed in the data with increasing x including a MS transition near $x = 0.35$, a monotonic decrease in the IR absorption band energy, and a maximum in the low-energy (< 4 eV) spectral weight near the MS transition. We show that these results are qualitatively consistent with a *bond-order* CDW picture that associates many of the bismuthate normal-state properties with the deviations of the Bi-O bond length from equilibrium.

II. EXPERIMENT

Single-crystal samples of $Ba_{1-x}K_xBiO_3$ were grown by a top-seeded electrochemical technique described elsewhere.[15] Since high temperature growth conditions are not required for the electrochemical process,[15] significantly higher potassium doping levels can be obtained than are possible with traditional synthesis methods.[16,17] In order to investigate the doping dependence of the optical response through the MS transition, measurements were made on three semiconducting samples with $x = 0.0$, 0.24, 0.31, and three superconducting samples with $x = 0.38$ ($T_c = 31.5$ K), $x = 0.41$ ($T_c = 30$ K), and $x = 0.51$ ($T_c = 21.5$ K). The K concentrations (x) were determined by x-ray diffraction. The superconducting transition temperatures (T_c) were obtained from the bulk magnetization results shown in Fig. 1. For the optical measurements, one of the large (approximately 1 mm $\times$ 1 mm) sample faces was mechanically polished to a mirrorlike surface using a 0.5 micron abrasive. All optical measurements were performed immediately after pol-

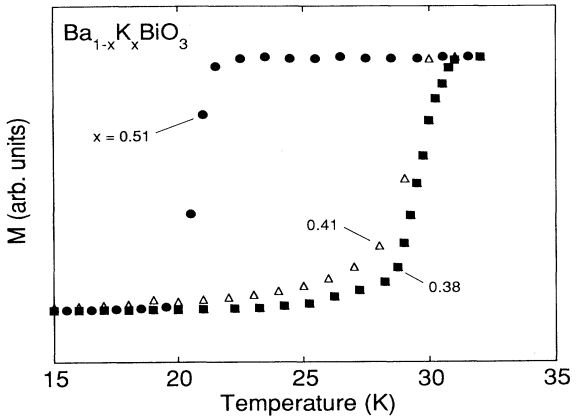

FIG. 1. Bulk magnetization (zero-field cooled) for the superconducting samples taken on warming. The data have been scaled to the magnetization at 5 K for each sample.

ishing to reduce the possibility of surface degradation due to atmosphere exposure.

The reflectance was measured with a rapid-scanning Fourier transform interferometer at near-normal incidence between 0.01 and 5 eV for the $x=0$ sample and between 0.1 and 5 eV for samples with $x\neq 0$. Several combinations of sources, beamsplitters, and detectors, with overlapping spectral regions, were used to cover this energy range. The data from overlapping spectral ranges never differed by more than 1%. The spectroellipsometric measurements were performed between 1.5 and 5.5 eV on a rotating analyzer system with an incident angle of roughly 66°. Spectroellipsometry is a self-normalizing technique and is, therefore, insensitive to surface imperfections (i.e., microscratches due to polishing). The measured reflectances and those calculated from the ellipsometric data agreed to within 3% in all cases, which confirms the consistency of our data.

By combining reflectance and spectroellipsometric data, it is possible to significantly reduce errors in the calculated optical constants which are introduced when the limited reflectivity data are extrapolated in a Kramers-Kronig[18] (KK) analysis. A detailed discussion of this correction procedure has been published previously,[19] so only a brief description will be given here. The first step of our correction procedure includes choosing a high-frequency extrapolation for the reflectivity such that the phase of the complex reflectance obtained from the KK transform matches the low-energy part of the ellipsometrically determined phase. Once this has been achieved, the KK derived phase is set equal to the ellipsometric phase above approximately 3 eV, forming the corrected phase, $\Theta_{\rm corr}(\omega)$. In order to take advantage of the ellipsometer's greater sensitivity at high energy, the measured reflectance is also equated with the ellipsometrically determined reflectance above approximately 3.5 eV, to form $R_{\rm Comb}(\omega)$. Finally, $R_{\rm Comb}(\omega)$ and $\Theta_{\rm corr}(\omega)$ are used in standard constitutive relations to calculate the optical constants. This procedure effectively eliminates the errors associated with traditional KK analyses, yielding optical constants that are exact to within experimental error over the entire measured energy range.

III. RESULTS AND ANALYSIS

The development of the optical reflectance with doping, x, is presented in Fig. 2 up to 4 eV. The most obvious trends as x increases are a monotonic increase of the reflectance in the infrared (IR) region and a monotonic decrease of the plasma energy. The reflectance between 2 and 5.5 eV is shown in the inset of Fig. 2. The optical response above 3.5 eV is nearly independent of x, indicating that the electronic states in this energy range are relatively insensitive to doping. Qualitatively similar reflectance results have been reported previously for film[13,20] and polycrystalline samples[14,21] ($x<0.4$), however, the low-frequency ($\omega<2$ eV) reflectance values exhibited by our single crystals are considerably larger than those previously reported.

The doping dependence of the real part of the optical conductivity, σ_1, obtained from our corrected KK analysis, is shown in Fig. 3 up to 4 eV. The most prominent features of σ_1 are (i) a strong absorption band in the infrared (hereinafter referred to as the "IR absorption band") which decreases in energy monotonically with increasing x, (ii) a large free-carrier absorption centered at zero frequency which develops for $x\geq 0.38$, and (iii) a deep minimum above the IR absorption band. The low-energy response of σ_1 indicates the presence of a MS transition near $x=0.35$ at room temperature. The IR absorption band in $BaBiO_3$ has been assigned to charge excitations across the CDW gap,[22–25] so the systematic decrease in the IR absorption band energy at higher doping levels suggests that the CDW gap energy, E_g, decreases monotonically with increasing x. It is noteworthy that the IR absorption band persists into the metallic regime ($x>0.35$), remaining resolvable as a shoulder on the free-carrier response for $x=0.38$ and 0.41. The conductivity minimum above the IR absorption band implies that the bands nearest the Fermi energy are well separated from the other bands.

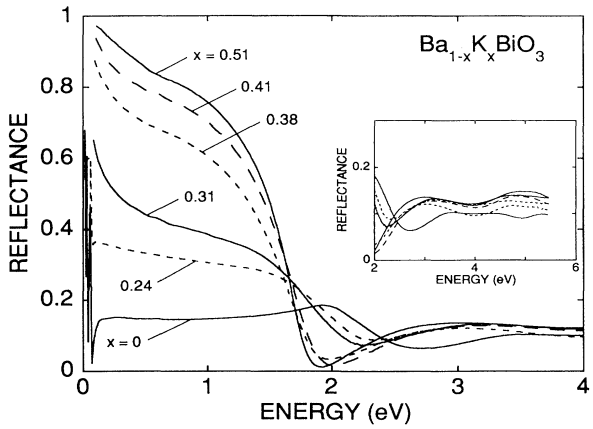

FIG. 2. Room-temperature optical reflectance of BKBO as a function of doping. The inset shows the higher-energy reflectance which is truncated in the main graph to emphasize the low-energy response.

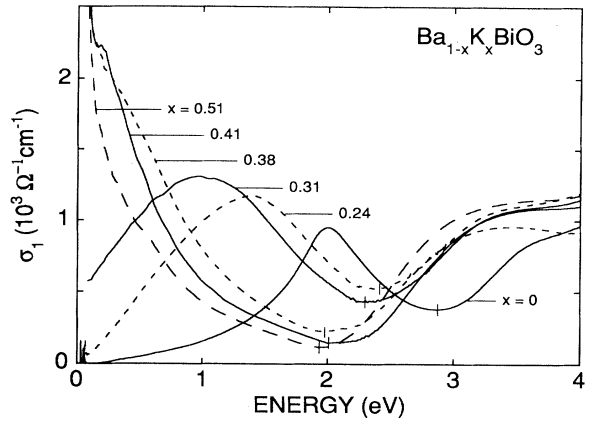

FIG. 3. The optical conductivity of BKBO, obtained by our corrected Kramers-Kronig procedure (Ref. 19), as a function of x. Vertical hash marks indicate the values of ω_0 used as the upper limit in the spectral weight integration of Eq. (1) (see Fig. 5).

The doping dependence of the integrated optical conductivity can be analyzed quantitatively by defining the spectra function, $N_{\text{eff}}(\omega)$, as

$$N_{\text{eff}}(\omega)=\frac{2mV_{\text{cell}}}{\pi e^2}\int_0^{\omega}\sigma_1(\omega')d\omega' , \quad (1)$$

where m and e are the free-electron mass and charge, respectively, and V_{cell} is the unit-cell volume. Comparison to the well-known f sum rule identifies the quantity $(m/m^*)N_{\text{eff}}(\omega)$ as the total effective number of carriers (free and bound) per unit cell participating in conduction below ω, where m^* is the renormalized (effective) carrier mass. An equivalent plasma frequency can be assigned to $N_{\text{eff}}(\omega)$ as follows:

$$\omega_p^2=\frac{4\pi e^2}{m}\frac{(m/m^*)N_{\text{eff}}(\omega)}{V_{\text{cell}}}=8\int_0^{\omega}\sigma_1(\omega')d\omega' . \quad (2)$$

Equation (2) emphasizes that $(m/m^*)N_{\text{eff}}(\omega)$ includes both bound and free-carrier contributions below ω, since

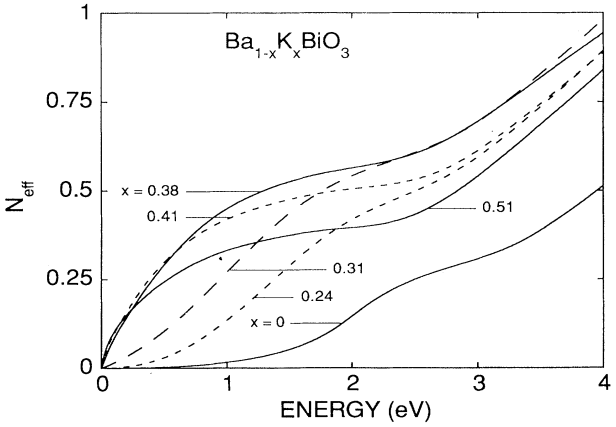

FIG. 4. The effective number of carriers, N_{eff}, obtained from an integration of the optical conductivity (Fig. 3) according to Eq. (1).

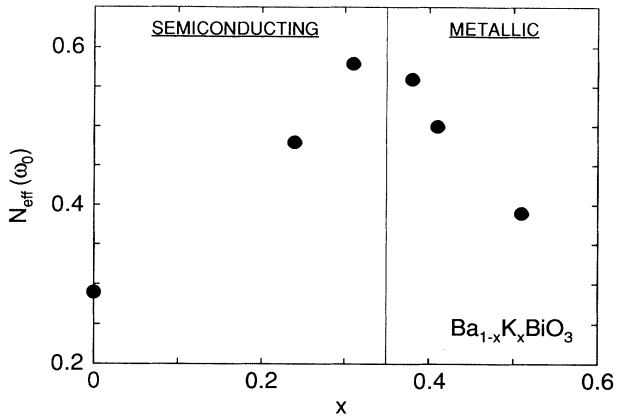

FIG. 5. The low-energy spectral weight obtained by integrating the optical conductivity (Fig. 3) up to the conductivity minimum, ω_0, plotted vs x.

ω_p^2 is defined in terms of the total integrated conductivity.

The optical conductivity in Fig. 3 was integrated according to Eq. (1) to obtain $N_{\text{eff}}(\omega)$ between 0 and 4 eV as shown in Fig. 4. The MS transition results in a clear difference between $N_{\text{eff}}(\omega)$ for $x \leq 0.31$, which increases slowly from zero at low energies and rises sharply when the IR absorption band is encountered, and $N_{\text{eff}}(\omega)$ for $x \geq 0.38$, which rises quickly from zero at low frequencies due to the large free-carrier component and plateaus in the vicinity of the conductivity minimum. Notably, as a function of increasing x, the magnitude of $N_{\text{eff}}(\omega)$ for all values of ω between 0 and 4 eV *increases* in the semiconducting regime, but *decreases* in the metallic regime, exhibiting a maximum near the MS transition. This unusual behavior is better illustrated in Fig. 5 where the integral of the optical conductivity between $\omega=0$ and the conductivity minimum, ω_0 (vertical hash marks in Fig. 3), is plotted versus x. Figure 5 indicates that the spectral weight associated with the bands nearest the Fermi energy reaches a maximum near the MS transition. We point out that the qualitative results presented in Fig. 5 do not depend significantly on the particular choice of ω_0, but that by choosing ω_0 in the conductivity minimum, the most accurate quantitative estimate is obtained. Unfortunately, the doping dependence of the free-carrier density cannot be accurately determined from the optical data because it is impossible to unambiguously separate the free-carrier and IR absorption band components of the spectral weight in the metallic regime.

IV. DISCUSSION

The principal optical results of the preceding section can be summarized as follows: (i) a MS transition occurs near $x=0.35$ at room temperature; (ii) the IR absorption band energy decreases monotonically with increasing x and persists into the metallic regime; and (iii) the integral of the optical conductivity below the conductivity minimum, $N_{\text{eff}}(\omega_0)$, *increases* with x in the semiconducting regime, but *decreases* with x in the metallic regime, reaching a maximum near the MS transition.

In view of the fact that substituting K for Ba removes electrons from the system, one possible interpretation of the $N_{\text{eff}}(\omega_0)$ results shown in Fig. 5 is that a crossover from holelike to electronlike carriers occurs near the MS transition with increasing x.[26] This interpretation is strongly supported by the available Hall and Seebeck effect results which indicate that the carriers are holes in $BaBiO_3$,[27,28] and electrons in $Ba_{0.6}K_{0.4}BiO_3$.[29,30] Additional doping-dependent transport measurements need to be performed in order to confirm the crossover point and to obtain the free-carrier density in the metallic regime.

The doping dependence of the optical data can be understood in the context of general theoretical arguments concerning the nature of the CDW state in the bismuthates. Given the small charge transfer between Bi sites[3,7,31–34] and the covalent nature of the Bi-O bond,[3,34] the appropriate CDW paradigm for the bismuthates is a *bond-order* CDW in which the charge density is associated with the inequivalent Bi-O bonds rather than with the Bi sites as in the so-called site-diagonal CDW picture (e.g., $Ba_2Bi^{3+}Bi^{5+}O_6$). Within the bond-order CDW picture, the BiO_3 lattice is unstable at half filling to a symmetric Peierls distortion that alternately expands and contracts the oxygen octahedra[3,7,35] as illustrated in Fig. 6. Such "breathing mode" distortions have, in fact, been observed in structural studies[1,36] of $BaBiO_3$. The CDW state is stable presumably because its electronic energy is lower than the energy of the undistorted state by an amount greater than or equal to the commensurate Peierls condensation energy, E_C. The Peierls distortion doubles the unit cell, which splits the half-filled metallic band [qualitatively illustrated in Fig. 7(a)] into filled and empty subbands [Fig. 7(b)],[37] resulting in a semiconducting ground state. The separation between the subbands is approximately equal to the CDW gap energy, E_g, which should depend to some extent on the magnitude of the deviation of the Bi-O bond length from equilibrium, u (Fig. 6).

Away from half filling, the CDW state should remain energetically favorable so long as the doped holes do not reduce the condensation energy per electron, E_C/N, below some critical fraction, f_c, of the CDW gap energy, E_g. Therefore, at small doping concentrations, electrons are removed from the top of the filled subband as illustrated in the schematic semiconducting band structure of Fig. 7(c). This is expected to result in a linearly increasing carrier (hole) density with increasing x, in agreement

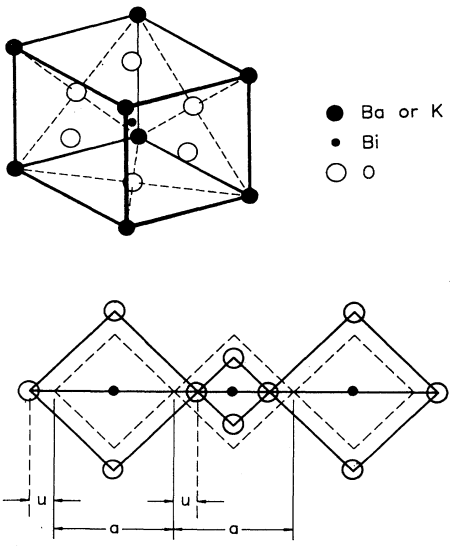

FIG. 6. The cubic perovskite structure of BKBO is shown for reference in the upper drawing. The lower drawing is a schematic representation of the oxygen octahedra. The solid lines illustrate the symmetric Peierls distortions and the dashed lines illustrate the undistorted case. The deviation of the Bi-O bond length from equilibrium, u, and the lattice spacing, a, are identified.

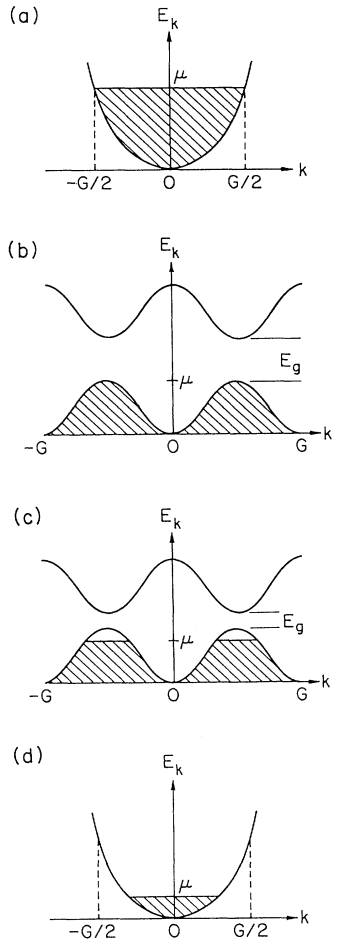

FIG. 7. A qualitative band structure derived from the bond-order CDW picture is illustrated (Ref. 12). (a) shows the half-filled metallic band apparent in the absence of a CDW distortion. The splitting of this half-filled band into filled and empty subbands by the CDW is shown in (b). (c) and (d) illustrate the effect of doping on the band structure for semiconducting (c) and metallic (d) cases. Below the MS transition (c), doping adds holes to the top of the filled subband, whereas above the MS transition (d), doping removes carriers from a $(1-x)/2$ filled band. The energy difference between the split bands in the semiconducting regime is the CDW gap energy, E_g.

with the doping dependence of N_{eff} in the semiconducting regime (Fig. 5). The MS transition occurs at approximately the doping level where $E_C/N \approx f_c E_g$.[35] The concomitant collapse of the CDW gap at the MS transition leads to a recombination of the split bands, resulting in a $(1-x)/2$ filled metallic band as illustrated in Fig. 7(d). In this case, doping is expected to decrease the free-carrier (electron) density linearly with increasing x. The observed behavior of N_{eff} in the metallic regime (Fig. 5) appears consistent with this prediction. It is important to remember, however, that Fig. 5 plots the total carrier density and that doping dependence of the free-carrier density is not known with certainty in the metallic regime.

Within the bond-order CDW picture (see Fig. 6), the systematic decrease in the IR absorption band energy with increasing x suggests a decrease in the Bi-O bond length distortion, u, with doping. Indeed, such a decrease in u has been observed in doping-dependent extended x-ray-absorption fine-structure (EXAFS) measurements.[31,33] A more quantitative comparison between the optical and EXAFS results can be made using a specific CDW gap equation proposed by Rice and Wang (RW) for BKBO:[35]

$$E_g = [\alpha^2 + 6(V+\gamma u)^2]^{1/2} - [\alpha^2 + 6(V-\gamma u)^2]^{1/2} . \quad (3)$$

In Eq. (3), α is the Bi $6s$ orbital energy, V is the $6s$-$2p$ hopping integral at the equilibrium Bi-O bond length, γ is the derivative of the hopping integral with respect to position along the Bi-O bond direction, and u is the magnitude of the Bi-O bond length distortion as shown in Fig. 6. Since the values[35] of $V \sim 2.2$ eV, $\alpha^2 \sim 1.21$ eV^2, and $\gamma \sim 5.1$ eV/Å are essentially independent of doping, Eq. (3) relates E_g directly to the Bi-O bond length distortion, u. Estimated values of the Bi-O bond length distortions, computed from Eq. (3), are $u = 0.08$ Å ($x = 0$), $u = 0.055$ Å ($x = 0.24$), and $u = 0.039$ Å ($x = 0.31$). These estimated u values compare favorably with the available EXAFS data in the semiconducting regime,[31,33] although there is not a one-to-one correspondence between the doping levels included in the various studies. Additional data, especially EXAFS data as a function of doping, is needed in order to fully verify the RW relation.

The persistence of the IR absorption band into the metallic regime is somewhat difficult to understand. For instance, phase separation (i.e., the presence of both metallic and semiconducting phases) is not a plausible explanation because the IR absorption band evolves smoothly with doping in the metallic regime. It is interesting to note, however, that the magnitude of the optically estimated Bi-O bond length distortion in the metallic regime [Fig. 3 and Eq. (3) lead to $u < 0.01$ Å for $x \geq 0.38$] falls below the EXAFS resolution. Thus, one possibility is that local static CDW distortions remain in the metallic regime which the absorption measurements are unable to detect. Another, and perhaps more probable, explanation is that the metallic regime is characterized by dynamic fluctuations in the CDW order. Not only would such local fluctuations be unobservable in standard structural investigations (except possibly diffuse x-ray scattering), they would also lack the spatial and temporal coherence necessary to sustain a pervasive semiconducting state.

It is natural at this point to compare the optical response of BKBO to that of BPBO. Although an analysis of the low-energy spectral weight has not been reported for BPBO, rough estimates of the integrated optical conductivity based on published data[23,38,39] appear consistent with a maximum near the MS transition. Also, the available Hall and Seebeck effect data for metallic BPBO indicate that, like BKBO, the charge carriers are electrons.[2,40] An interesting contrast between the two materials is that the IR absorption band energy decreases much more slowly with doping in BPBO (Refs. 23, 38, and 39) than in BKBO. When interpreted in terms of a bond-order CDW picture, this suggests the existence of finite Bi-O bond length distortions at higher doping levels in BPBO. Unfortunately, the resiliency of local distortions in BPBO compared to BKBO is not well understood. It has recently been suggested that K doping screens the CDW charge fluctuations more effectively than Pb doping, but this is difficult to justify since holes are added to the O $2p$ band regardless of the dopant site.[32,41,42] Furthermore, since the bands at the Fermi surface have partial Bi character, the screening due to Pb doping should, if anything, be more effective.

Our results emphasize the coupling between the electronic state and local structural distortions in the bismuthates. It is noteworthy that structural distortions modulate absorption bands in a number of other cubic transition-metal oxide perovskites as well. For instance, recent optical investigations[43] of the charge-transfer insulators, $RTiO_3$ (R = La, Ce, Pr, Nd, Sm, Gd), show a mid-IR band whose energy position increases with decreasing Ti-O-Ti bond angle (La→Gd). Another example is the Mott-Hubbard $RNiO_3$ (R = La, Pr, Nd, Sm, Eu, Y, Lu) system[44] in which a decrease in the Ni-O-Ni bond angle with rare earth (La→Lu) leads to a metal-to-semiconductor transition between La and Pr, and an increasing band-gap energy in the semiconducting regime. The correspondence between these results is rather striking, especially given the significantly different origins of the semiconductivity in these three systems. In the case of the nickelates and the titanates, the energy gap is determined by the width of the Hubbard bands which narrows with decreasing bond angle.[43,44] By contrast, the magnitude of the Bi-O bond length distortion appears to govern the CDW gap energy in the bismuthates. Thus, it is clear that a connection exists between local structural distortions and the electronic state of a variety of cubic transition-metal oxide perovskites, although the specific nature of the coupling is different.

We note finally that although the well-known "midinfrared" band in the high-T_c cuprates bears a certain superficial resemblance to the IR absorption band in the bismuthates, there are significant differences between the optical responses of these materials. First, in the bismuthates, the IR absorption band evolves continuously from the fundamental CDW absorption band at $x = 0$. By contrast, in the cuprates, the midinfrared band coexists with the fundamental charge-transfer absorption band at intermediate doping.[19,45] This indicates that the effect of dop-

ing on the electronic structure is completely different in these two systems. In addition, contrary to previous conclusions,[20] we find that the frequency dependence of the optical response below the plasma energy is distinctly different in the bismuthates and the cuprates, and that there is no evidence for a universal low-frequency normal-state response among the high-T_c superconductors.

V. SUMMARY

The experimental data we present in this paper represent the first single-crystal reflectance data for BKBO, and cover a sufficiently wide range of doping ($0 \leq x \leq 0.51$) to critically test theoretical predictions regarding the effects of doping through the MS transition. Our results show that with increasing x, a MS transition occurs near $x = 0.35$, the CDW gap energy decreases monotonically, and the integrated optical conductivity reaches a maximum near the MS transition. The development of the low-energy spectral weight with doping suggests a crossover from holelike to electronlike conduction at the MS transition, consistent with the available Hall and Seebeck effect data. A self-consistent interpretation of these results is given within the bond-order CDW picture in which deviations of the Bi-O bond length from equilibrium influence many aspects of the bismuthate normal state. In particular, the doping dependence of the integrated optical conductivity is consistent with a simple band structure derived from the bond-order CDW picture, and the CDW gap energy is directly related to the magnitude of the Bi-O bond length distortions. A comparison of our results with the optical response of other cubic transition-metal oxide perovskites suggests the possibility of a fundamental connection between the IR absorption bands observed in these materials and local structural distortions. Finally, we note that there is currently no evidence to support a connection between the IR absorption band in the bismuthates and the "midinfrared" band in the high-T_c cuprates.

ACKNOWLEDGMENTS

This work was supported by the National Science Foundation under Grant No. NSF DMR 91-20000 through the Science and Technology Center for Superconductivity. Partial support for M.A.K. was provided by the Department of Defense.

*Present address: 3M Center, Bldg. 60-1S-13, St. Paul, MN 55144.

[1]S. Pei, J. D. Jorgensen, B. Dabrowski, D. G. Hinks, D. R. Richards, A. W. Mitchell, J. M. Newsam, S. K. Sinha, D. Vaknin, and A. J. Jacobson, Phys. Rev. B **41**, 4126 (1990).

[2]T. D. Thanh. A. Koma, and S. Tanaka, Appl. Phys. **22**, 205 (1980).

[3]L. F. Mattheiss and D. R. Hamann, Phys. Rev. B **28**, 4227 (1983).

[4]L. F. Mattheiss and D. R. Hamann, Phys. Rev. Lett. **60**, 2681 (1988).

[5]A. Bansil and S. Kaprzyk, Phys. Rev. B **43**, 10 335 (1991).

[6]D. A. Papaconstantopoulos, A. Pasturel, J. P. Julien, and F. Cyrot-Lackmann, Phys. Rev. B **40**, 8844 (1989).

[7]L. F. Mattheiss and D. R. Hamann, Phys. Rev. B **26**, 2686 (1982).

[8]W. Weber, Proceedings of the 18th International Conference on Low Temperature Physics [Jpn. J. Appl. Phys. **26**, Suppl. 3, 981 (1987)].

[9]D. Yoshioka and H. Fukuyama, J. Phys. Soc. Jpn. **54**, 2996 (1985).

[10]T. M. Rice and L. Sneddon, Phys. Rev. Lett. **47**, 689 (1981).

[11]E. Juarczek and T. M. Rice, Europhys. Lett. **1**, 225 (1986).

[12]N. V. Anshukova, A. I. Golovashkin, L. I. Ivanova, and A. P. Rusakov, Sverkhprovodimost' (KIAE) **5**, 644 (1992) [Superconductivity **5**, 644 (1992)].

[13]H. Sato, S. Tajima, H. Takagi, and S. Uchida, Nature **338**, 241 (1989).

[14]S. H. Blanton, R. T. Collins, K. H. Kelleher, L. D. Rotter, Z. Schlesinger, D. G. Hinks, and Y. Zheng, Phys. Rev. B **47**, 996 (1993).

[15]P. D. Han, L. Chang, and D. A. Payne, J. Cryst. Growth **128**, 798 (1993).

[16]R. J. Cava, B. Batlogg, J. J. Krajewski, R. Farrow, L. W. Rupp, Jr., A. E. White, K. Short, W. F. Peck, and T. Kometani, Nature **332**, 814 (1988).

[17]D. G. Hinks, B. Dabrowski, J. D. Jorgensen, A. W. Mitchell, D. R. Richards, S. Pei, and D. Shi, Nature **333**, 836 (1988).

[18]F. Stern, *Solid State Physics* (Academic, New York, 1963), Vol. 15.

[19]S. L. Cooper, D. Reznik, A. L. Kotz, M. A. Karlow, R. Liu, M. V. Klein, W. C. Lee, J. Giapintzakis, D. M. Ginsberg, and B. W. Veal, Phys. Rev. B **47**, 8233 (1993).

[20]I. Bozovic, J. H. Kim, J. S. Harris, Jr., E. S. Hellman, E. H. Hartford, and P. K. Chan, Phys. Rev. B **46**, 1182 (1992).

[21]Z. Schlesinger, R. T. Collins, J. A. Calise, D. G. Hinks, A. W. Mitchell, Y. Zheng, B. Dabrowski, N. E. Bickers, and D. J. Scalapino, Phys. Rev. B **40**, 6862 (1989).

[22]S. Uchida, S. Tajima, A. Masaki, S. Sugai, K. Kitazawa, and S. Tanaka, J. Phys. Soc. Jpn. **54**, 4395 (1985).

[23]S. Uchida, K. Kitazawa, and S. Tanaka, Phase Transition **8**, 95 (1987).

[24]K. F. McCarty, H. B. Radousky, D. G. Hinks, Y. Zheng, A. W. Mitchell, T. K. Folkerts, and R. N. Sheton, Phys. Rev. B **40**, 2662 (1989).

[25]S. Tajima, M. Yoshida, N. Koshizuka, H. Sato, and S. Uchida, Phys. Rev. B **46**, 1232 (1992).

[26]We point out that similar transitions have been observed in $La_{2-z}Sr_zCuO_4$ and $Nd_{2-z}Ce_zCuO_4$ at the superconductor-to-normal-metal boundary, although there is no evidence that the transition in the bismuthates and these cuprates have similar origins. [S. Uchida, H. Takagi, Y. Tokura, N. Koshihara, and T. Arima, in *Strong Correlation and Superconductivity,* edited by H. Fukuyama, S. Maekawa, and A. P. Malozemoff (Springer-Verlag, Berlin, 1989), p. 194.]

[27]F. Munakata, A. Nozaki, T. Kawano, and H. Yamauchi, Solid State Commun. **83**, 355 (1992).

[28]H. Takagi, S. Uchida, S. Tajima, K. Kitazawa, and S. Tanaka,

Proceedings of the 18th International Conference on the Physics of Semiconductors (World Scientific, Singapore, 1986), p. 1851.

[29]M. Sato, S. Kondoh, and M. Sera, in *Strong Correlation and Superconductivity* (Ref. 26), p. 341.

[30]C. Uher, S. D. Peacor, and A. B. Kaiser, Phys. Rev. B **43**, 7955 (1991).

[31]S. M. Heald, D. DiMarzio, M. Croft, M. S. Hegde, S. Li, and M. Greenblatt, Phys. Rev. B **40**, 8828 (1989).

[32]M. S. Hegde, P. Barboux, C. C. Chang, J. M. Tarascon, T. Venkatesan, X. D. Wu, and A. Inam, Phys. Rev. B **39**, 4752 (1989).

[33]S. Salem-Sugui, Jr., E. E. Alp, S. M. Mini, M. Ramanathan, J. C. Campuzano, G. Jennings, M. Faiz, S. Pei, B. Dabrowski, Y. Zheng, D. R. Richards, and D. G. Hinks, Phys. Rev. B **43**, 5511 (1991).

[34]Z.-X. Shen, P. A. P. Lindberg, B. O. Wells, D. S. Dessau, A. Borg, I. Lindau, W. E. Spicer, W. P. Ellis, G. H. Kwei, K. C. Ott, J.-S. Lang, and J. W. Allen, Phys. Rev. B **40**, 6912 (1989).

[35]M. J. Rice and Y. R. Wang, Physica C **157**, 192 (1989).

[36]D. E. Cox and A. W. Sleight, Solid State Commun. **19**, 969 (1976); Acta Crystallogr. B **35**, 1 (1979).

[37]A similar band structure to that illustrated in Fig. 7 has been presented (Ref. 12) in conjunction with another qualitative model for the BKBO normal-state properties. We reiterate, however, that this band structure arises from very general arguments which are independent of the details of any specific model.

[38]S. Tajima, S. Uchida, A. Masaki, H. Takagi, K. Kitazawa, S. Tanaka, and A. Katsui, Phys. Rev. B **32**, 6302 (1985).

[39]S. Tajima, S. Uchida, A. Masaki, H. Takagi, K. Kitazawa, S. Tanaka, and S. Sugai, Phys. Rev. B **35**, 696 (1987).

[40]T. Tani, T. Itoh, and S. Tanaka, Proceedings of the 15th International Conference on the Physics of Semiconductors [J. Phys. Soc. Jpn. **49**, Suppl. A, 309 (1980)].

[41]M. W. Ruckman, D. Di Marzio, Y. Jeon, G. Liang, J. Chen, M. Croft, and M. S. Hegde, Phys. Rev. B **39**, 7359 (1989).

[42]G. K. Wertheim, J. P. Remeika, and D. N. E. Buchanan, Phys. Rev. B **26**, 2120 (1982).

[43]D. A. Crandles, T. Timusk, J. D. Garrett, and J. E. Greedan, Physica C **201**, 407 (1992).

[44]J. B. Torrance, P. Lacorre, A. I. Nazzal, E. J. Ansaldo, and Ch. Niedermayer, Phys. Rev. B **45**, 8209 (1992).

[45]S. L. Cooper, A. L. Kotz, M. A. Karlow, M. V. Klein, W. C. Lee, J. Giapintzakis, and D. M. Ginsberg, Phys. Rev. B **45**, 2549 (1992).